

Salvia miltiorrhiza monomer IH764-3 induces hepatic stellate cell apoptosis via caspase-3 activation

Xiao-Lan Zhang, Li Liu, Hui-Qing Jiang

Xiao-Lan Zhang, Li Liu, Hui-Qing Jiang, Department of Gastroenterology, The Second Hospital of Hebei Medical University, Shijiazhuang 050000 Hebei Province, China

Supported by Fund of the Scientific and Technical Department of Hebei Province, No. 01276134

Correspondence to: Professor Hui-Qing Jiang, Department of Gastroenterology, The Second Hospital of Hebei Medical University, Shijiazhuang 050000, Hebei Province, China. huiqingj@heinfo.net
Telephone: +86-311-7046901 Ext. 6513

Received 2001-12-20 Accepted 2002-01-23

Abstract

AIM: To investigate the effects of IH764-3 on HSC apoptosis, and the expression of caspase-3 protein in HSC apoptotic process.

METHODS: HSCs were cultured in medium with different IH764-3 doses ($10\mu\text{g}\cdot\text{mL}^{-1}$, $20\mu\text{g}\cdot\text{mL}^{-1}$, $30\mu\text{g}\cdot\text{mL}^{-1}$, $40\mu\text{g}\cdot\text{mL}^{-1}$) and without IH764-3, and HSC proliferation was quantitatively measured by ^3H -thymidine incorporation. The morphological changes of HSCs were observed with transmission electron microscope after exposure to the dose of $40\mu\text{g}\cdot\text{mL}^{-1}$ of IH764-3 for 48 hr. The apoptosis rates were detected by annexin V/PI and TdT-mediated dUTP nick end labeling (TUNEL). The expression of caspase-3 protein was determined by flow cytometry.

RESULTS: (1) HSC proliferation rates induced with different IH764-3 doses ($10\mu\text{g}\cdot\text{mL}^{-1}$, $20\mu\text{g}\cdot\text{mL}^{-1}$, $30\mu\text{g}\cdot\text{mL}^{-1}$, $40\mu\text{g}\cdot\text{mL}^{-1}$) were significantly reduced compared with that of the control group ($P < 0.01$). (2) With the doses above, IH764-3 dose-dependently produced HSC apoptosis rates of 6.7% (9.4%), 9.3% (21.6%), 15.1% (27.2%) and 19.0% (28.4%) respectively, by annexin V and PI-labeled flow cytometry assay (or TUNEL), while it was only 2.3% (6.7%) in the control. (3) The expression of caspase-3 protein in IH764-3 groups was significantly higher than that of the control ($P < 0.05$).

CONCLUSION: Within the dose range used in present study, IH764-3 can inhibit HSC proliferation, as well as enhance HSC apoptosis. Furthermore, IH764-3 can significantly increase the caspase-3 protein expression.

Zhang XL, Liu L, Jiang HQ. Salvia miltiorrhiza monomer IH764-3 induces hepatic stellate cell apoptosis via caspase-3 activation. *World J Gastroenterol* 2002;8(3):515-519

INTRODUCTION

Hepatic fibrosis occurs as a result of the accumulation of excess extracellular matrix (ECM) around the hepatic sinus and portal vein^[1-19]. Activated hepatic stellate cells (HSCs) are the main source of ECM in the process of hepatic fibrosis. Therefore, HSCs play a central role in the hepatic fibrogenesis^[20-34]. Either proliferation or apoptosis of HSCs or both may affect the population of HSCs^[35-39]. Recent studies have shown that apoptosis is the main process to eliminate the activated HSCs during the resolution of hepatic fibrosis^[40-42]. To induce the apoptosis of HSCs, therefore, might be an

important strategy for the hepatic fibrosis therapy^[43-45].

Chinese herbal medicine *Salviae Miltiorrhiza*, which can improve circulatory status and eliminate stasis, exhibits a series of important pharmacological effects on anti-inflammation, antioxidation, and inhibiting the platelet aggregation^[46-49]. IH764-3, extracted from *Salviae Miltiorrhiza*, preserves all of these beneficial effects. Furthermore, in recent studies, it has been documented that IH764-3 could play an important role in anti-fibrosis, inhibiting the proliferation of HSCs and the synthesis of collagens^[47,50]. However, there are few reports so far concerns about the effects of IH764-3 on HSC apoptosis and its mechanisms. In present study, we therefore used annexin-V/PI double labeling flow cytometry, TUNEL and transmission electron microscope to examine the effects of IH764-3 on HSC apoptosis. Meanwhile, the effects of IH764-3 on the expression of caspase-3 protein during HSC apoptosis were also observed.

MATERIALS AND METHODS

Materials

HSC line CFSC was established and kindly provided by Prof. Greenwel in America, which phenotype was activated HSCs, and derived from the CCl_4 -induced cirrhotic rat^[51]. RPMI-1640 medium was purchased from GIBCOL Co. Fetal calf serum was from Four Season Green Biological Co, Hangzhou, China. IH764-3 was kindly provided by Prof. Chun-Zheng Yang from Hematopathy Institute, Chinese Academy of Medical Science. ^3H -TdR was from Isotope Institute, Chinese Academy of Atomic Energy. Annexin-V cell apoptosis assay kit was purchased from Baosai Biological Technology Co, Beijing. TUNEL assay kit was from Boster Biological Engineering Co, Wuhan, China. Caspase-3 assay kit was from CLONTECH Co, USA. Goat anti-mouse FITC-IgG was the product of Microorganism Institute, Academy of Military Medical Sciences, China. Other reagents were analytically pure.

Methods

Cell culture The HSCs were thawed and plated in RPMI-1640 medium containing $100\text{mL}\cdot\text{L}^{-1}$ fetal calf serum, $100\text{KU}\cdot\text{L}^{-1}$ penicillin, $100\text{mg}\cdot\text{L}^{-1}$ streptomycin, $4\text{mmol}\cdot\text{L}^{-1}$ L-glutamine and $0.1\text{mmol}\cdot\text{L}^{-1}$ HEPES. Cells were kept in culture at 37°C in a $50\text{mL}\cdot\text{L}^{-1}$ CO_2 atmosphere and 100% humidity. The HSCs were digested with 0.25% trypsin and subcultured from one to three when the cells proliferated into a full monolayer. The first change of the culture medium was made about 24 hr after subculturing, and then the cells were subcultured again about 72 hr. Experiments were carried out while the cells were in exponential growth phase. Cells were plated in 25cm^2 plastic flasks at a density of $2\times 10^5\cdot\text{L}^{-1}$ or onto 96-well plates at a density of $5\times 10^6\cdot\text{L}^{-1}$. When the cells were nearly 100% confluent, they were continued to incubate for another 12 hr in serum-free RPMI-1640 culture medium. At that time most of the cells were in G_0 phase, they were divided into different groups. The dose-response studies were performed using different doses of IH764-3 ($10\mu\text{g}\cdot\text{mL}^{-1}$, $20\mu\text{g}\cdot\text{mL}^{-1}$, $30\mu\text{g}\cdot\text{mL}^{-1}$ and $40\mu\text{g}\cdot\text{mL}^{-1}$) and lasted for 12-48 hr, while the time-response studies were carried out at the timepoints of 12, 24, 48 and 72 hr with the dose of $30\mu\text{g}\cdot\text{mL}^{-1}$ of IH764-3.

Inhibition of cell proliferation assays HSCs were plated to triplicate wells in a 96-well plate with the concentration of $5 \times 10^3 \cdot \text{mL}^{-1}$. When the cells were nearly 100% confluent, they were cultured in serum-free medium for 12 hr. Then the medium was replaced with fresh medium containing 2% fetal calf serum and different IH764-3 doses, $1.11 \times 10^4 \text{ Bq } ^3\text{H-Thymidine}$ was added to each well. After 24 hr of incubation, HSCs were collected onto filter membrane and baked 1 hr at 100°C . The radioactivity (cpm) was determined with the beta-scintillation counter (Beckman). The inhibition of HSC proliferation was expressed by inhibitory rate, which was calculated as: inhibition rate = [(cpm of control group - cpm of IH764-3 group) / cpm of control group] $\times 100\%$.

Apoptosis detection The following methods were used to detect apoptosis: (1) Transmission electron microscope: After exposure to the dose of $40 \mu\text{g} \cdot \text{mL}^{-1}$ of IH764-3 for 48 hr, cells were trypsinized, collected, washed with PBS and centrifuged at 1200g for 10 min. The cell pellet was fixed in 4% glutaral for 2 hr, 1% osmium acid for 1 hr and dehydrated gradually, then stained by uranium acetic acid and lead citromalic acid. The cells were observed with transmission electron microscope and the ultrastructural changes were recorded. (2) Annexin-V/PI labeling to detect apoptotic rate^[52]: Briefly, the trypsinized HSCs were washed twice with PBS, stained with annexin-V (10L) and PI ($5 \mu\text{L}$) for 10 min, and the apoptotic rate was quantified by FACSCalibur flow cytometry (Becton Dickinson Inc.) at 488 nm wavelength. More than 1×10^4 cells were detected, and the results were analyzed with Modfit LT software. The stained cells were divided into three subgroups: The cells in V⁻/PI⁻ subgroup were survived cells which membrane was intact, The cells in V⁺/PI⁻ subgroup were apoptotic cells which membrane intact but with phosphatidylserine translocation; The cells in V⁺/PI⁺ subgroup were necrotic cells which membrane was impairment and with phosphatidylserine translocation. (3) Determination of apoptosis by TUNEL method: After trypsinization and collection, cells were fixed with 4% paraformaldehyde for 30 min. Apoptosis was assayed by TUNEL method. Briefly, the cells were incubated with proteinase K ($5 \mu\text{L} \cdot \text{mL}^{-1}$) at 37°C for 5 min, labeled by TdT and digoxin-d-UTP at 4°C in a humidified chamber to stay overnight, anti-digoxin antibody was added. After being incubated at 37°C for 30 min, the cells were stained with diaminobenzidine (DAB). Apoptotic cells presented as brownish stain in the nucleus, but we should pay special attention to distinguish the stained DNA fragments in cytoplasm due to some nuclear leakage. At least 500 cells were examined and the rate of apoptotic cells was calculated as the percentage of stained-cell per 100 cells.

Determination of Caspase-3 expression Trypsinized cells were washed in PBS, and fixed at 4°C in 70% ethanol overnight. Fixed cells were precipitated and washed in PBS. Cells (6×10^5) were suspended in 0.5 mL permeable buffer diluted by PBS, and subsequently incubated with anti-Caspase-3 antibody, FITC-labeled goat anti-rat IgG antibody (1:20)^[53], then cells were washed with PBS, assayed by flow cytometer. The relative quantity of the protein was expressed by Fluorescence index (FI).

Statistical analysis

Data were expressed as $\bar{x} \pm s$. One-way analysis of variance was used for multiple comparisons, and Newman-Keuls test and χ^2 test were used for intra-groups comparisons. *P* values less than 0.05 were considered to be statistically significant.

RESULTS

Effect of IH764-3 on proliferation of HSCs

Compared with the control group, IH764-3 had a significant inhibitory effect on $^3\text{H-TdR}$ incorporation; the inhibition was dose-dependent (Table 1).

Table 1 The effect of IH764-3 on $^3\text{H-TdR}$ incorporation ($\bar{x} \pm s$)

Dosage ($\mu\text{g} \cdot \text{mL}^{-1}$)	Cpm	Inhibitory rate (%)
0	19749 \pm 7222	
1	018339 \pm 5344	7.1
2	014147 \pm 1850 ^b	28.4
3	09125 \pm 916 ^b	53.8
4	05313 \pm 426 ^b	73.1

^b*P* < 0.01 vs control

Morphological changes

The shape of cells incubated with $30 \mu\text{g} \cdot \text{mL}^{-1}$ or $40 \mu\text{g} \cdot \text{mL}^{-1}$ of IH764-3 for 6 hr changed from stellate or shuttle to spherical, and the intercellular space was increased. 12 hr later, the cells began to detach from the plate and it is more remarkable at 24 hr. With the transmission electron microscope, the decreased volume, condensed chromatin and decreased nucleo-cytoplasmic ratio of apoptotic cell were noted. Some cells showed typical apoptotic changes: the pyknosis and margination of the nuclear chromatin. Moreover, the nuclei fragment, annular or crescent body, cytoplasm vacuoles and swollen Mitochondria were also observed. Some cells were karyolysis and turn into the specific apoptotic bodies (Figure 1).

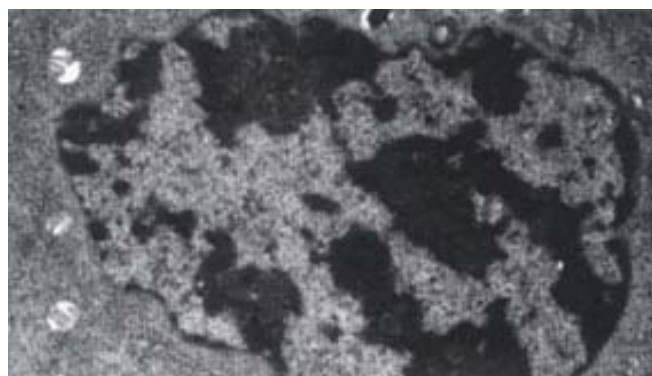


Figure 1 The apoptotic cells in $40 \mu\text{g} \cdot \text{mL}^{-1}$ IH764-3 for 48 hr (TEM 10000 \times) Apoptotic cells became small, the chromatin condensed

Annexin-V/PI combined labeling flow cytometry

The rate of apoptosis was both dose-dependent and time-dependent (Table 2A, 2B). For the $40 \mu\text{g} \cdot \text{mL}^{-1}$ group at 24 hr and $30 \mu\text{g} \cdot \text{mL}^{-1}$ group at 48-72 hr, the apoptotic cells presented worse progressive changes, most of the cells were V⁺/PI⁺ subclass, namely necrosis. The necrotic rate was 21.0-31.3%. Figure 2A, 2B.

Table 2A Apoptotic rates of HSCs exposed IH764-3 with different doses by Annexin-V/PI (%)

Time	doses				
	$0 \mu\text{g} \cdot \text{mL}^{-1}$	$10 \mu\text{g} \cdot \text{mL}^{-1}$	$20 \mu\text{g} \cdot \text{mL}^{-1}$	$30 \mu\text{g} \cdot \text{mL}^{-1}$	$40 \mu\text{g} \cdot \text{mL}^{-1}$
12hr	0.3	2.2	3.7	6.7	15.1
48hr	2.3	6.7	9.3	15.1	19.7

Table 2B Percentage of apoptotic HSCs exposed to IH764-3 ($30 \mu\text{g} \cdot \text{mL}^{-1}$) at different timepoints by Annexin-V/PI (%)

Time	0hr	12hr	24hr	48hr	72hr
Apoptosis rate	0.3	6.7	10.3	15.1	19.6

Detection of HSC apoptosis by TUNEL

After exposure of HSCs to different dose of IH764-3, the apoptotic indexes in experimental group by TUNEL assay at 48 hr were 9.4%

$\pm 2.6\%$ ($10\mu\text{g}\cdot\text{mL}^{-1}$), $21.6\% \pm 5.5\%$ ($20\mu\text{g}\cdot\text{mL}^{-1}$), $27.2\% \pm 6.2\%$ ($30\mu\text{g}\cdot\text{mL}^{-1}$) and $28.4\% \pm 6.5\%$ ($40\mu\text{g}\cdot\text{mL}^{-1}$), respectively, which were significantly higher than that in control group ($6.7\% \pm 0.6\%$, $P < 0.01$) (Figure 3).

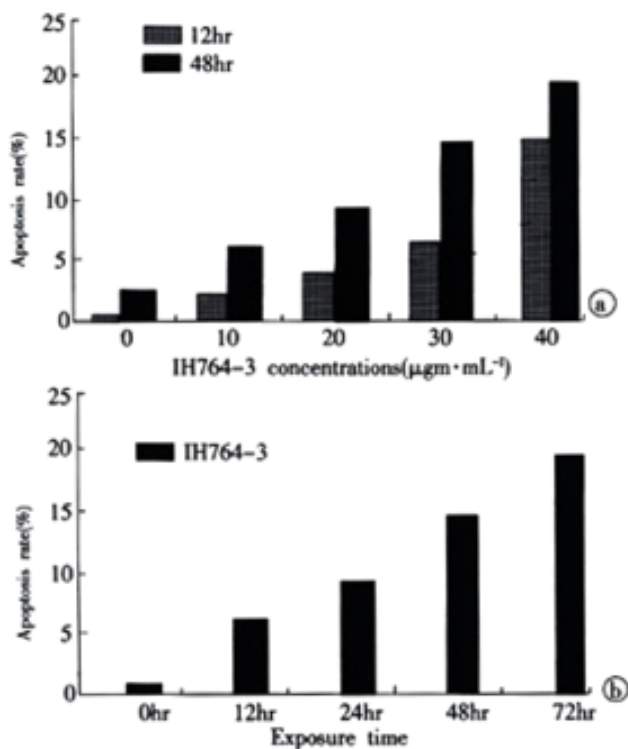


Figure 2 apoptosis rates of HSCs exposed to IH764-3. (A) dose-dependent; (B) time-dependent with the concentration of $30\mu\text{g}\cdot\text{mL}^{-1}$ of IH764-3.

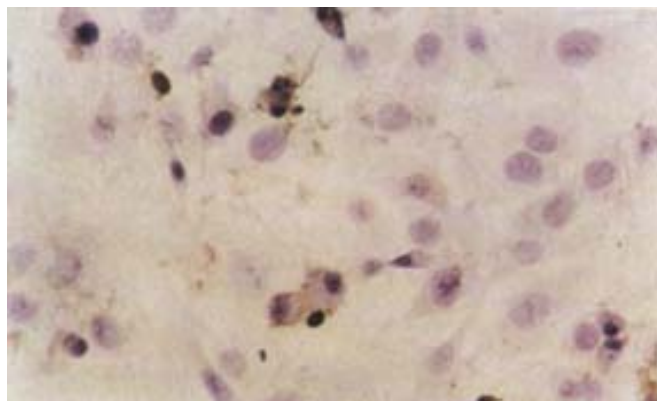


Figure 3 The apoptotic cells in $30\mu\text{g}\cdot\text{mL}^{-1}$ IH764-3 for 48hr (TUNEL10 \times 40)

IH764-3 induced caspase-3 protein Expression in HSCs

With the given doses, IH764-3 could increase Caspase-3 protein expression dose-dependently. There was also a positive relationship between Caspase-3 protein expression and apoptosis rate (Table 3).

Table 3 Fluorescence index of caspase-3 protein in HSCs ($\bar{x} \pm s$)

Dosage ($\mu\text{g}\cdot\text{mL}^{-1}$)	Caspase-3	P value
0	175.6 \pm 22.5	
10	215.1 \pm 26.9	<0.01
20	231.6 \pm 28.6	<0.01
30	304.7 \pm 30.7	<0.01
40	338.9 \pm 32.1	<0.01

DISCUSSION

The dynamic balance between the cell proliferation and apoptosis plays a key role in growth, development and maintenance of physiological functions of individuals. Once the balance is broken, varieties of pathological and pathophysiological changes will take place. HSCs are the major cells that produce ECM components and proliferated significantly in hepatic fibrosis^[56]. It has been considered that apoptosis may play at least a partial role in reducing HSC population and decreasing the production of ECM components in hepatic fibrosis, thus triggering the process of HSC apoptosis is perhaps an important strategy to resolve the hepatic fibrosis^[45,54]. IH764-3, an extract of *Salviae Miltiorrhiza*, has been proved to be an effective agent for anti-hepatic fibrosis in animal model. However, up to the present, whether its anti-fibrotic mechanism was related to the induction of HSC apoptosis or not has not been elucidated yet.

Cell apoptosis, which is different from necrosis, is an initiative cell death process that activates endogenous DNA endonuclease, with the morphological characteristics of pyknosis and the chromatin margination to become lump or crescent bodies. Then cytoplasm condenses and cell shrinks, which finally forms apoptotic bodies. However, the cell membrane is integrated and the organelles keep intact. In present study, a great deal of typical apoptotic cells was found on plates treated with IH764-3, which demonstrated that IH764-3 did trigger the HSC apoptosis.

Apoptosis is a dynamic developing process that can be divided into early phase, metaphase and late phase. It has been reported that flow cytometry is the most sensitive method to examine apoptosis^[52,53]. In early apoptotic phase, the translocation of phosphatidylserine, which has high affinity to Annexin-V, from the inner leaflet to the outer layer of the plasma membrane, could be easily recognized by Annexin-V labeling method. Moreover, when combining with PI stain, it could also distinguish from necrotic cells. In this study, we found that IH764-3 could dose-dependently induce apoptosis at 12 and 48 hr timepoints, the apoptotic rate was 2.2% in $10\mu\text{g}\cdot\text{mL}^{-1}$ group and 15.1% in $40\mu\text{g}\cdot\text{mL}^{-1}$ group. In $30\mu\text{g}\cdot\text{mL}^{-1}$ group, the apoptotic rate was time-dependent. In $40\mu\text{g}\cdot\text{mL}^{-1}$ group at 24hr and $30\mu\text{g}\cdot\text{mL}^{-1}$ group at 48-72hr, the apoptotic cells presented progressive worse advanced changes, most of the cells became necrotic, the necrotic rate reached 21.0-31.3%. Similar changes were also observed with transmission electron microscope. Thus it could be concluded that low doses of IH764-3 mainly induced apoptosis, while in high doses, it could not only induce apoptosis, but also necrosis.

The remarkable biochemical characteristic of apoptosis is the genome DNA fragmentation. This is because the activated endogenous endonuclease can degrade the connected DNA between nucleosomes into 180-200bp oligonucleotide fragments. With terminal deoxynucleotidyl transferase, utilizing exogenous biotin-labeled-free nucleotides, the free nucleotides in 3' terminal can be catalyzed to get together in a non template-dependent manner, making the break nicks of DNA is labeled. Therefore, we used TUNEL method as another way to prove the apoptosis further. The results showed that apoptosis indexes in IH764-3 groups were higher than that of the control. Furthermore, the indexes were dose-dependent in IH764-3 groups. All of the above demonstrated that IH764-3 could induce HSC apoptosis in time and dose-dependent manner, but the signal transduction process remains unclear.

Caspase-3, a key proteinase in apoptosis pathway, is one of the proteases in cysteine aspartic acid specific proteases family, and is also called as cysteine proteases P32. It splits the peptide bond at asparagic residue of specific motif sequence in substrate protein. The activated caspase-3 may cause apoptosis^[55] and results in what we saw the apoptotic signs under microscope. Caspase-3 can split inhibitory caspase activated deoxyribonuclease (ICAD) into CAD^[56,57], which

degrades DNA in nucleus.

To examine the possible mechanism of HSC apoptosis induced by IH764-3, we observed the expression of caspase-3 protein. The results showed that IH764-3 from $10\mu\text{g}\cdot\text{mL}^{-1}$ to $40\mu\text{g}\cdot\text{mL}^{-1}$ could increase the expression of caspase-3 protein. The more the apoptosis developed, the more the caspase-3 protein expressed. So we deduced that HSC apoptosis induced by IH764-3 was mediated by caspase-3 activation. Increased expression of caspase-3 protein was possibly one of the mechanisms in HSC apoptosis induced by IH764-3. Any reagents that increase caspase-3 protein expression might have a potential possibility to become new drugs to treat patients with hepatic fibrosis^[58].

ACKNOWLEDGEMENTS

The authors wish to thank Professor Greenwel for his kindly providing the cell line and Professor Chun-zheng Yang for presenting IH764-3. We also thank Dr Hong-Qun Liu and Dr Shuang Chen for their critical reading of the manuscript.

REFERENCES

- Jiang HQ, Zhang XL. Progress in the study of pathogenesis in hepatic fibrosis. *Shijie Huaren Xiaohua Zazhi* 2000;8:687-689
- Wu CH. Fibrodynamics-elucidation of the mechanisms and sites of liver fibrogenesis. *World J Gastroenterol* 1999;5:388-390
- Wang JY, Zhang QS, Guo JS, Hu MY. Effects of glycyrrhetic acid on collagen metabolism of hepatic stellate cells at different stages of liver fibrosis in rats. *World J Gastroenterol* 2001;7:115-119
- Du WD, Zhang YE, Zhai WR, Zhou XM. Dynamic changes of type α_1 , III and IV collagen synthesis and distribution of collagen-producing cells in carbon tetrachloride-induced rat liver fibrosis. *World J Gastroenterol* 1999;5:397-403
- Friedman SL. Molecular mechanisms of hepatic fibrosis and principles of therapy. *J Gastroenterol* 1997;32:424-430
- Shapiro SD, Senior RM. Matrix metalloproteinase: matrix degradation and more. *Am J Respir Cell Mol Biol* 1999;20:1100-1102
- Massova I, Kotra LP, Fridman R, Mobashery S. Matrix metalloproteinases: structure, evolution, and diversification. *FASEB J* 1998;12:1075-1095
- Benyon RC, Hovell CJ, Gaca MD, Jones EH, Iredale JP, Arthur MJ. Progelatinase A is produced and activated by rat hepatic stellate cells and promotes their proliferation. *Hepatology* 1999;30:977-986
- Knittel T, Mehde M, Kobold D, Saile B, Dinter C, Ramadori G. Expression patterns of matrix metalloproteinases and their inhibitors in parenchymal and non-parenchymal cells of rat liver: regulation by TNF- α and TGF- β 1. *J Hepatol* 1999;30:48-60
- Bai WY, Yao XX, Feng LY. The study status of liver fibrosis. *Shijie Huaren Xiaohua Zazhi* 2000;8:1267-1268
- Bahr MJ, Vincent KJ, Arthur MJ, Fowler AV, Smart DE, Wright MC, Clark IM, Benyon RC, Iredale JP, Mann DA. Control of the tissue inhibitor of metalloproteinases-1 promoter in culture-activated rat hepatic stellate cells: regulation by activator protein-1 DNA binding proteins. *Hepatology* 1999;29:839-848
- Liu HL, Li XH, Wang DY, Yang SP. Matrix metalloproteinase-2 and tissue inhibitor of metalloproteinase-1 expression in fibrotic rat liver. *World J Gastroenterol* 2000;6:881-884
- Greenwel P, Dominguez-Rosales JA, Mavi G, Rivas-Estilla AM, Rojkind M. Hydrogen peroxide: a link between acetaldehyde-elicited α_1 (I) collagen gene up-regulation and oxidative stress in mouse hepatic stellate cells. *Hepatology* 2000;31:109-116
- Friedman SL. Cytokines and fibrogenesis. *Semin Liver Dis* 1999;19:129-140
- Weng HL, Cai WM, Liu RH. Animal experiment and clinical study of effect of gamma-interferon on hepatic fibrosis. *World J Gastroenterol* 2001;7:42-48
- Yao XX. Diagnosis and treatment of hepatic fibrosis. *Shijie Huaren Xiaohua Zazhi* 2000;8:681-689
- Xiang DD, Li QF, Wang YM, Wang YF. The effect of vitamin E emulsion on procollagen III and matrix metalloproteinases-1 mRNA in hepatic stellate cells. *Shijie Huaren Xiaohua Zazhi* 1999;7:1085
- Svegliati-Baroni G, Ridolfi F, Di Sario A, Saccomanno S, Bendia E, Benedetti A, Greenwel P. Intracellular signaling pathways involved in acetaldehyde-induced collagen and fibronectin gene expression in human hepatic stellate cells. *Hepatology* 2001;33:1130-1140
- Chen PS, Zhan WR, Zhang YE, Zhang JS. The effect of hypoxia on collagen and matrix metalloproteinase hepatic stellate cells. *Shijie Huaren Xiaohua Zazhi* 2000;8:586-587
- Pinzani M, Marra F, Carloni V. Signal transduction in hepatic stellate cells. *Liver* 1998;18:2-13
- Huang GC, Zhang JS. Signal transduction in activated hepatic stellate cells. *Shijie Huaren Xiaohua Zazhi* 2001;9:1056-1060
- Carloni V, Pinzani M, Giusti S, Romanelli RG, Parola M, Bellomo G, Failli P, Hamilton AD, Sebt SM, Laffi G, Gentilini P. Tyrosine phosphorylation of focal adhesion kinase by PDGF is dependent on ras in human hepatic stellate cells. *Hepatology* 2000;31:131-140
- Zhu YH, Hu DR. The establishment and application of hepatic stellate cell lines. *Shijie Huaren Xiaohua Zazhi* 1999;7:348-349
- Zhu YH, Hu DR, Nie QH, Liu GD, Tan ZX. Study on activation and c-fos, c-jun expression of *in vitro* cultured human hepatic stellate cells. *Shijie Huaren Xiaohua Zazhi* 2000;8:299-302
- Huang GC, Zhang JS, Zhang YE. Effects of retinoic acid on proliferation, phenotype and expression of cyclin-dependent kinase inhibitors in TGF- β 1-stimulated rat hepatic stellate cells. *World J Gastroenterol* 2000;6:819-823
- Potter JJ, Rennie-Tankersley L, Anania FA, Mezey E. A transient increase in c-myc precedes the transdifferentiation of hepatic stellate cells to myofibroblast-like cells. *Liver* 1999;19:135-144
- Xiang DD, Wei YL, Li QF. Molecular mechanism of transforming growth factor β 1 on Ito cell. *Shijie Huaren Xiaohua Zazhi* 1999;7:980-981
- Lu LG, Zeng MD, Li JQ, Qiu DK, Hua J, Fan ZP. Expression of intercellular adhesion molecule-1 and hepatic stellate cell activation. *Shijie Huaren Xiaohua Zazhi* 1998;6:567-569
- Tang YW, Yao XX. The regulated role of Hepatocarcinoma cell in hepatic stellate cell activation. *Shijie Huaren Xiaohua Zazhi* 2001;9:202-204
- Huang X, Li DG, Wang ZR, Wei HS, Cheng JL, Zhan YT, Zhou X, Xu QF, Li X, Lu HM. Expression changes of activin A in the development of hepatic fibrosis. *World J Gastroenterol* 2001;7:37-41
- Liu C, Liu P, Liu CH, Zhu XQ, Ji G. Effects of Fuzhenghuayu decoction on collagen synthesis of cultured hepatic stellate cells, hepatocytes and fibroblasts in rats. *World J Gastroenterol* 1998;4:548-549
- Wei HS, Lu HM, Li DG, Zhan YT, Wang ZR, Huang X, Cheng JL, Xu QF. The regulatory role of AT 1 receptor on activated HSCs in hepatic fibrogenesis: effects of RAS inhibitors on hepatic fibrosis induced by CCl₄. *World J Gastroenterol* 2000;6:824-828
- Vasilidou V, Lee J, Pappa A, Petersen DR. Involvement of p65 in the regulation of NF- κ B in rat hepatic stellate cells during cirrhosis. *Biochem Biophys Res Commun* 2000;273:546-550
- Kato R, Kamiya S, Ueki M, Yajima H, Ishii T, Nakamura H, Katayama T, Fukui F. The fibronectin-derived antiadhesive peptides suppress the myofibroblastic conversion of rat hepatic stellate cells. *Exp Cell Res* 2001;265:54-63
- Lu P, Luo HS, Yu BP. Apoptosis and liver diseases. *Shijie Huaren Xiaohua Zazhi* 2000;8:1157-1159
- Gressner AM. The cell biology of liver fibrogenesis-an imbalance of proliferation, growth arrest and apoptosis of myofibroblasts. *Cell Tissue Res* 1998;292:447-452
- Liu WB, Wang JY. NF- κ B and apoptosis of hepatic stellate cells. *Shijie Huaren Xiaohua Zazhi* 2001;9:1054-1055
- Lang A, Schoonhoven R, Tuvia S, Brenner DA, Rippe RA. Nuclear factor kappa B in proliferation, activation, and apoptosis in rat hepatic stellate cells. *J Hepatol* 2000;33:49-58
- Saile B, Matthes N, Knittel T, Ramadori G. Transforming growth factor β and tumor necrosis factor β inhibit both apoptosis and proliferation of activated rat hepatic stellate cells. *Hepatology* 1999;30:196-202
- Gong W, Pecci A, Roth S, Lahme B, Beato M, Gressner AM. Transformation-dependent susceptibility of rat hepatic stellate cells to apoptosis induced by soluble Fas ligand. *Hepatology* 1998;28:492-502
- Iwamoto H, Sakai H, Tada S, Nakamura M, Nawata H. Induction of apoptosis in rat hepatic stellate cells by disruption of integrin-mediated cell adhesion. *J Lab Clin Med* 1999;134:83-89
- Iredale JP, Benyon RC, Pickering J, McCullen M, Northrop M, Pawley S, Hovell C, Arthur MJ. Mechanisms of spontaneous resolution of rat liver fibrosis. Hepatic stellate cell apoptosis and reduced hepatic expression of metalloproteinase inhibitors. *J Clin Invest* 1998;102:538-549
- Fischer R, Schmitt M, Bode JG, Haussinger D. Expression of the peripheral-type benzodiazepine receptor and apoptosis induction in hepatic stellate cells. *Gastroenterology* 2001;120:1212-1226
- Issa R, Williams E, Trim N, Kendall T, Arthur MJ, Reichen J, Benyon RC, Iredale JP. Apoptosis of hepatic stellate cells: involvement in resolution of biliary fibrosis and regulation by soluble growth factors. *Gut* 2001;48:548-557
- Cales P. Apoptosis and liver fibrosis: antifibrotic strategies. *Biomed Pharmacother* 1998;52:259-263
- Yang CZ, Liu RL, Liu J. The role of IH764-3 in prolyl hydroxyl of

- collagen biosynthesis. *Zhongguo Yixue Kexueyuan Xuebao* 1993;15:364-368
- 47 Wasser S, Ho JM, Ang HK, Tan CE. Salvia Miltiorrhiza reduces experimentally induced hepatic fibrosis in rats. *J Hepatol* 1998;29:760-771
- 48 Liu CH, Hu YY, Wang XL, Liu P, Xu LM. Effects of salvianolic acid-A on NIH/3T3 fibroblast proliferation, collagen synthesis and gene expression. *World J Gastroenterol* 2000;6:361-364
- 49 Cheng ML, Liu SD. The basic study and clinical research on hepatic fibrosis. 1st ed. Beijing: People's Medical Publishing House 1996:228-283
- 50 Chen YX, Li S, Fan LY, Kong XT, Yang CZ, Yu BL. The experiment study of effect on hepatic fibrosis by Salvia Miltiorrhiza monomer IH764-3. *Zhonghua Yixue Zazhi* 1998;78:636-637
- 51 Greenwel P, Schwartz M, Rossas M, Peyrol S, Grimaud JA, Rojkind M. Characterization of fat-storing cell lines derived from normal and CCl₄-cirrhotic livers. *Lab Invest* 1991;65:644-653
- 52 Boersma AW, Nooter K, Oostrum RG, Stoter G. Quantification of apoptotic cells with fluorescein isothiocyanate-labeled annexin V in chinese hamster ovary cell cultures treated with cisplatin. *Cytometry* 1996;24:123-130
- 53 Zuo LF. Flow cytometry and biomedicine. *Shenyang: Liaoning Sci Technol Publ House* 1996;213-267
- 54 Iredale JR. Hepatic Stellate Cell Behavior during Resolution of Liver Injury. *Semin Liver Dis* 2001;21:427-436
- 55 Nagata S. Apoptosis by death factor. *Cell* 1997;88:355-365
- 56 Enari M, Talianian RV, Wong WW, Nagata S. Sequential activation of ICE-like and CPP32-like proteases during Fas-mediated apoptosis. *Nature* 1996;380:723-726
- 57 Sakahira H, Enari M, Nagata S. Cleavage of CAD inhibitor in CAD activation and DNA degradation during apoptosis. *Nature* 1998;391:96-99
- 58 Wright MC, Issa R, Smart DE, Trim N, Murray GI, Primrose JN, Arthur MJP, Iredale JP, Mann DA. Gliotoxin Stimulates the Apoptosis of Human and Rat Hepatic Stellate Cells and Enhances the Resolution of Liver Fibrosis in Rats. *Gastroenterology* 2001;121:685-698

Edited by Zhu L